World Academy of Science, Engineering and Technology
International Journal of Materials and Metallurgical Engineering
Vol:6, No:5, 2012

The Surface Adsorption of Nano-pore Template

M. J. Kao, S.F. Chang, C.C. Chen*, C.G. Kuo*

Abstract**—**This paper aims to fabricated high quality anodic aluminum oxide (AAO) film by anodization method. AAO pore size, pore density, and film thickness can be controlled in 10~500 nm, 10^8~10^{11} pore . cm^{-2}, and 1~100 μm. AAO volume and surface area can be computed based on structural parameters such as thickness, pore size, pore density, and sample size. Base on the thetorical calculation, AAO has 100 μm thickness with 15 nm, 60 nm, and 500 nm pore diameters AAO surface areas are 1225.2 cm^2, 3204.4 cm^2, and 549.7 cm^2, respectively. The large unit surface area which is useful for adsorption application. When AAO adsorbed pH indictor of bromphenol blue presented a sensitive pH detection of solution change. This testing method can further be used for the precise measurement of biotechnology, convenience measurement of industrial engineering.

Keywords**—**AAO, Pore, Surface area, Adsorption, Indicator

I. Introduction

RECENT estimates by several research institutes suggest that by the year 2015, $1 trillion worth of products worldwide will incorporate nanotechnology in key functional components. Roco [1] identifies four generations of nanotechnology products: passive nanostructures (circa 2000), active nanostructures (circa 2005), systems of nanosystems (circa 2010), and molecular nanosystems (circa 2015-2020). During the first generation, the emphasis was more on discovery and production of nanostructures. In the second generation, the focus has shifted towards devices and complex nanosystems. Nanostructures play a fundamental role in nanotechnology research, especially in the development of nanosystems. In addition, nanostructures such as nanotubes and nano film have also played an important role in the applied research community. For example, TiO_2 film has received much attention for solar cell energy generation [2-3]. Carbon nanotube film can be applied for LCD backlighting [4] and flexible transistor arrays [5]. Anodic Aluminum Oxide film for drug released [6].

Honeycomb structures with high aspect ratios on the nanometer scale have received interest for various applications. To obtain an array nanochannel as a template, nanoporous alumina formed by anodization has widely been studied several decades [7-9]. Aluminum in the presence of air or aqueous electrolytes is always covered with a thin natural layer of alumina.

M.J. Kao, Department of Industrial Education, National Taiwan Normal University, Taipei, 10643, Taiwan (lilikao25@hotmail.com)

S.F. Chang, Department of Industrial Education, National Taiwan Normal University, Taipei, 10643, Taiwan (shaofu78@gmail.com)

C.C. Chen. Department of Energy Engineering, National United University, Miaoli 36003, Taiwan (phone: +886-37-382383; fax:+886-37-382-391; e-mail: chentexas@gmail.com).

C.G. Kuo, Department of Industrial Education, National Taiwan Normal University, Taipei, 10643, Taiwan (chinguo7@yahoo.com.tw)

When a positive voltage is applied to an aluminum substrate in a suitable electrolyte, pores form on the surface at almost random positions. However, under specific conditions, almost perfect hexagonally ordered pores in anodic alumina can be obtained. Anodic aluminum oxide (AAO) has received much attention, because of its application to the preparation of templates and host materials for fabricating nanometer-scale devices including magnetics, electronics, optoelectronics, bio-sensing and engineered catalytic devices. Electrolytes such as chromic acid (CrO_3; 2.5~3%, 40 V, 40°C), sulfuric acid (H_2SO_4; 15~20%, 14~22 V, 18~25°C), oxalic acid ($C_2H_2O_4$; 5~10%, 50~65 V, 30°C), boric acid (H_3BO_3; 9~15%, 50~500 V, 90~95°C), and phosphoric acid (H_3PO_4; 10%, 10~12 V, 23~25°C) for AAO fabrication have been commonly mentioned in most reports [10-13]. Numerous researchers have focused on the high purity (99.999%) of an aluminum substrate, the control of applied voltage, electrolyte pH, and the composition of the solution, pore widening and compensation processes to fabricate a regular array of nanopores on an alumina film. A process which requires a high purity of aluminum (99.999%) and two-step anodization is expensive [14-18]. The principal methods of fabricating nanochannels include AAO, conventional photolithography-base techniques, and direct-write electron-beam lithography. However, the fabrication of structures with feature sizes smaller than 100 nm is a rather daunting task using the conventional electron beam and photolithographic techniques.

The arrayed nano-pores cannot be easily obtained unless highly pure (above 99.999%) aluminum foils are used. The anodized oxide film includes two layers; the outer layer is thicker and more porous than the inner layer. The inner layer is also named the barrier, active or dielectric layer and usually represents 0.1 to 2% of the thickness of the entire film. [19] Akahori [20] has studied that the melting point of this inner oxide layer is 1000°C, lower than that of bulk alumina (2017°C for Al_2O_3). Consequently, self-diffusion occurs in the nanochannel when the temperature reaches 700°C. The spacing of the nano-channels can be controlled to some extent by varying process conditions, such as the type, concentration, and temperature of the electrolytic solution used for anodic oxidation, and the amount of voltage applied. For example, varying voltage during the AAO process results in different channel sizes. The relationship between the spacing 2R (nm) of the narrow pores and the anodic oxidation voltage V (volts) can be characterized by the empirical relationship $2R=10+2V$. Another equation, $C=mV$, can be used to characterize the relationship between pore size C (nm) and anodic oxidation voltage V (volts), where m is a constant (2.0~2.5).

II. Experimental Procedure

Aluminum foil (1070, 99.7%) with dimensions $3cm^2$ × 0.3mm was put inside the electrochemical holder forming AAO through electrolyte polishing and anodization in electrochemical bath. The topography of the electro-polish Al surface was elucidated by optical microscopy (OM). The surfaces were then anodized for 3 hr at 40 V using platinum plate as the counter electrode in 3 wt.% oxalic acid ($C_2H_2O_4$) electrolyte at 20 ^oC.

As described in Chen [11-13, 21], AAO film can be fabricated using an anodization process. The fabrication processes for 15 nm AAO template consists of the following steps:

i. Polish the aluminum (Al) substrate (99.7%); then anneal in an air furnace at 550 ^oC.
ii. Electro-polish the substrate in a bath consisting of $HClO_4$, C_2H_6O, and $CH_3(CH_2)_3OCH_2CH_2OH$ with 42 V DC for 10 minutes.
iii. First anodization – Polish the Al substrate with 18 V DC in H_2SO_4 solution for 20 minutes.
iv. Remove the first anodization film by soaking in a solution of CrO_3 and H_3PO_4 for 40 minutes.
v. Second anodization – Repeat anodization using the solution from the first anodization, but for a longer time (several hours) to form AAO films of varying thickness.
vi. Remove Al substrate by soaking in a solution of $CuCl_2$ and HCl for 30 minutes.
vii. Widen pore diameter of AAO template using 5vol.% H_3PO_4 solution for 20 minutes.

According to above steps when the voltage and electrolyte (step **iii**) are change to 40V and 3 wt.% $C_2H_2O_4$, and pore widening time is 70 min (step **vii**), that 60 nm pore size of AAO can be formed. As well as, when the voltage and electrolyte (step **iii**) are change to 195V and 1 vol.% H_3PO_4, and pore widening time is 200 min (step **vii**), that 300 nm pore size of AAO can be formed. The topographies of the obtained AAO were observed using a JEOL JSM-6500F SEM (scanning electron microscopy)

To evaluate AAO adsorption property, the AAO samples were immersion in the 0.05wt.% bromphenol blue indicator for a period time at room temperature. The characteristics of AAO samples with indicator adsorption were test in by the acid and basic solutions.

III. Results And Discussion

A pH indicators for example, bromophenol blue ($C_{19}H_{10}Br_4O_5S$), methyl red ($C_{15}H_{15}N_3O_2$), methyl blue ($C_{37}H_{27}N_3O_9S_3.Na_2$) (Fig. 1), methylene blue trihydrate ($C_{16}H_{18}ClN_3S$) is a chemical detector for hydronium ions or hydrogen ions in the solution or vapor. For applications requiring the pH indicator paper or precise measurement of pH meter is frequently used. However, the inevasible used of pH indicator paper and an electrode volume limited of pH meter restrict to the application of pH indicators.

AAO film of different sizes, pore diameter, and thickness can be produced by varying parameter values such as voltage, time, and solution. For example, AAO with 10 nm to 25 nm pore size and 10μm/h film growth rate can be made by anodization of 10 vol.% H_2SO_4 electrolyte and 18V applied voltage, AAO with 30 nm to 90 nm pore size and 8μm/h film growth rate can be made by anodization of 3 wt.% $C_2H_2O_4$ electrolyte and 40V applied voltage, AAO with 180 nm to 500 nm pore size and 5μm/h film growth rate can be made by anodization of 1 vol.% H_3PO_4 electrolyte and 195V applied voltage. Fig. 2 showed SEM images of AAO pore size forming under electrolyte, applied voltage, and pore widening time controlling; (a)10 nm and (b) 20 nm were fabricated by 10 vol.% H_2SO_4 electrolyte, 18 V; (c) 30 nm, (d) 50nm, (e) 70 nm were fabricated by 3 wt.% $C_2H_2O_4$ electrolyte, 40V; (f) 250 nm, (g) 350 nm, and (h) 500 nm were fabricated by 1 vol.% H_3PO_4 electrolyte, 120~195V.

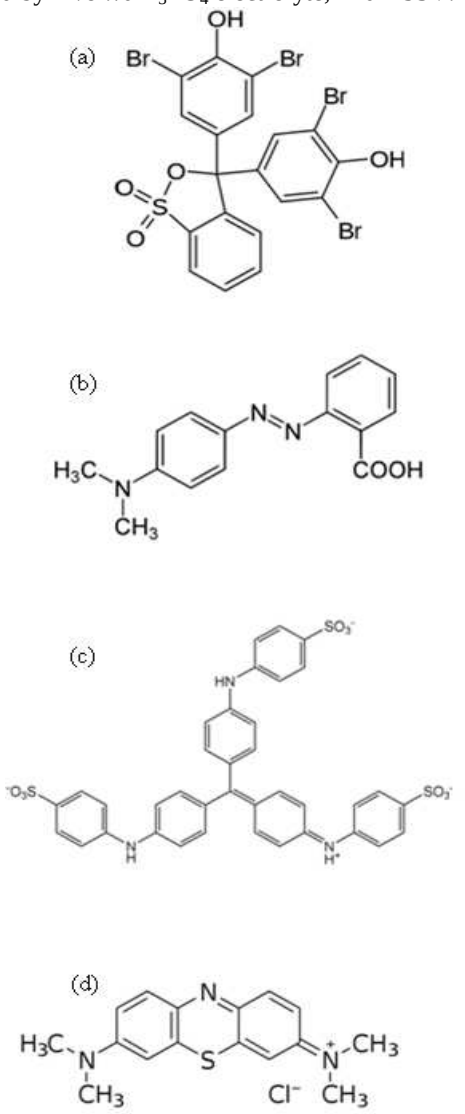

Fig. 1 The color indicator molecules structure; (a) bromophenol blue ($C_{19}H_{10}Br_4O_5S$), (b) methyl red ($C_{15}H_{15}N_3O_2$), (c) methyl blue ($C_{37}H_{27}N_3O_9S_3.Na_2$), (d) methylene blue trihydrate ($C_{16}H_{18}ClN_3S$)

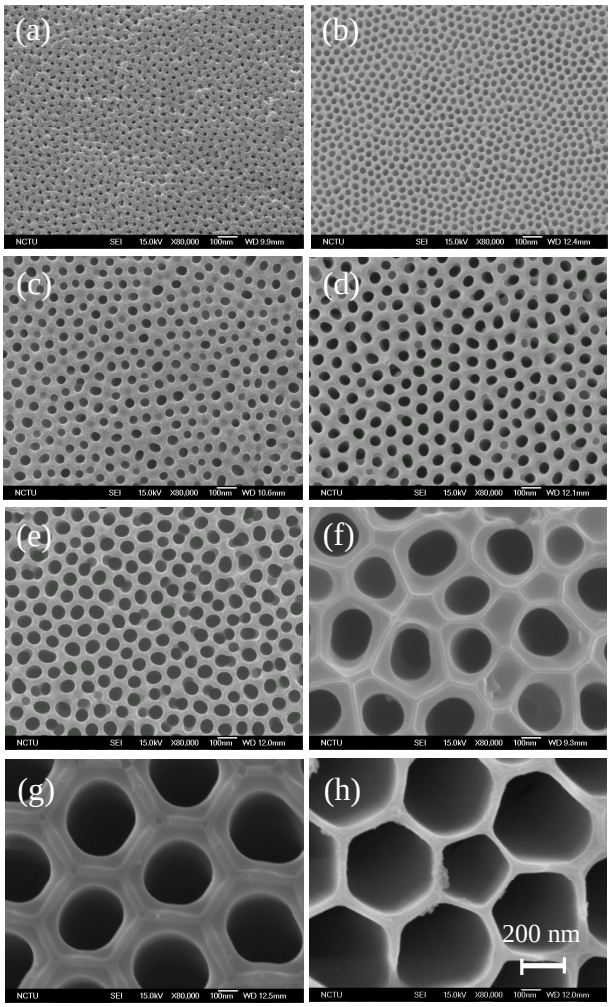

Fig. 2 SEM images of AAO pore size of (a)10 nm and (b)20 nm were fabricated by 10 vol.% H_2SO_4 electrolyte; (c) 30 nm, (d) 50nm, and (e) 70 nm were fabricated by 3 wt.% $C_2H_2O_4$ electrolyte; (f) 250 nm, (g) 350 nm, and (h) 500 nm were fabricated by 1 vol.% H_3PO_4 electrolyte

AAO surface area can be computed based on structural parameters such as thickness (D), pore size(2R), pore density(ρ), and sample size. For example, given three types of AAO with pore diameters of 15 nm, 60 nm, and 500 nm, the pore density can be computed as 2.6×10^{11}, 1.5×10^{10}, and 1.5×10^{8} pore/cm^2 when the pores are formed in order on the AAO. Fig. 3 showed the schematic The schematic diagram to evaluate the pore density(pores . cm^{-2}) and pore area fraction (%) on the AAO surface; (a) 15nm (1.8×10^{11} Pore density/ pores . cm^{-2}, 15.8%), (b) 60nm (1.3×10^{10} Pore density/ pores . cm^{-2}, 36.7%), (c) 85nm (1.0×10^{10} Pore density/ pores . cm^{-2}, 56.7%), (d) 100nm (7.6×10^{9} Pore density/ pores . cm^{-2}, 59.6%), (e) 200nm (2.1×10^{9} Pore density/ pores . cm^{-2}, 65.6%), (f) 300nm (1.0×10^{9} Pore density/ pores . cm^{-2}, 70.1%), (g) 400nm (6.0×10^{8} Pore density/ pores . cm^{-2}, 75.4%), (h) 500nm (4.7×10^{8} Pore density/ pores . cm^{-2}, 92.2%).; surface area with varied AAO pore size and film thickness can be calculated using the formulas $2\pi R \times D \times \rho$, based on a 1cm^2 sample area. The surface of AAO is increased in a unit volume. For example, when AAO has 100μm thickness with 15 nm, 60 nm, and 500 nm pore diameters AAO surface areas are 1225.2cm^2, 3204.4cm^2, and 549.7cm^2, respectively. Indeed, when AAO has 1cm thickness with 15 nm, 60 nm, and 500 nm pore diameters that AAO surface areas are 1,225,220cm^2, 320,442cm^2, 54,997cm^2, respectively. That means if an 1 cm^3 (surface area is 6cm^2) sample has AAO structure the surface areas can increase to 204,203, 53,407, and 9,166 times.

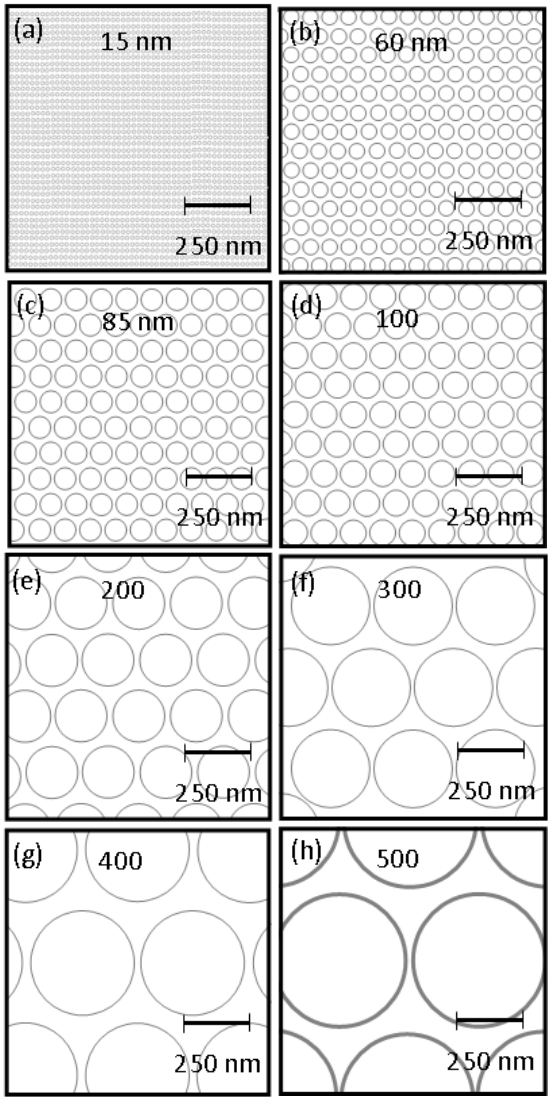

Fig. 3 The schematic diagram to evaluate the pore density(pores . cm^{-2})and pore area fraction (%) on the AAO surface; (a) 15nm (1.8×10^{11} Pore density/ pores . cm^{-2}, 15.8%), (b) 60nm (1.3×10^{10} Pore density/ pores . cm^{-2}, 36.7%), (c) 85nm (1.0×10^{10} Pore density/ pores . cm^{-2}, 56.7%), (d) 100nm (7.6×10^{9} Pore density/ pores . cm^{-2}, 59.6%), (e) 200nm (2.1×10^{9} Pore density/ pores . cm^{-2}, 65.6%), (f) 300nm (1.0×10^{9} Pore density/ pores . cm^{-2}, 70.1%), (g) 400nm (6.0×10^{8} Pore density/ pores . cm^{-2}, 75.4%), (h)500nm (4.7×10^{8} Pore density/ pores . cm^{-2}, 92.2%).

To evaluate AAO adsorption property, the AAO samples were immersion in the 0.05wt.% bromphenol blue indicator for a period time at room temperature. The characteristics of AAO samples with indicator adsorption were test in by the acid and basic solutions and the removal bromphenol blue indicator from AAO were tested by acetone dissolution and heating decomposition. Fig. 4 shows optical images of AAO surface colors. AAO surface can easily adsorb bromophenol blue solution. The adsorption quantity is controlled by adsorption time. Fig. 4(a) shows blue color with AAO adsorbs bromophenol blue solution for a short time. When increases adsorption time the bromophenol blue can be adsorbed on AAO in saturation. Fig. 4(b) shows dark blue color with AAO absorbs bromophenol blue solution for a long time.

Bromophenol blue is an organic substance that can be used as an analytical reagent. Based on its physical and chemical properties, bromophenol blue does not degrade quickly in the environment and is expected to be persistent in water and soil. Bromphenol blue pH indicator can changes from yellow to blue over the pH range 3.0 to 4.6 but, dissolution in a dilute basic solution. Fig. 4(c) shows yellow color with AAO/ bromophenol blue tested in the acid solution. Fig.e 4(d) shows light blue color with AAO/ bromophenol blue tested in the soap water of basic solution, the partial of bromophenol blue was desolated in the soap water. Bromphenol blue can be decomposed in the strong acid or strong basic solution; however, the AAO also dissolution in the strong acid or strong basic solution. In order to protect and re-use AAO the bromphenol blue was removed by acetone dissolution. Fig. 4(e) shows light yellow color with bromophenol blue removed by acetone dissolution and presented a cleaned AAO surface. The other remove bromphenol blue from AAO is by heating. Because bromphenol blue can be decomposed above 300℃ the AAO is stable above 300°C. Fig. 4(f) shows gray color with bromophenol blue removed by heating and presented a cleaned AAO surface.

IV. Conclusion

AAO surface area with varied AAO pore size and film thickness can be calculated using the formulas $2\pi R \times D \times \rho$, based on a $1cm^2$ sample area. The surface of AAO is increased in a unit volume. When AAO has 1cm thickness with 15 nm, 60 nm, and 500 nm pore diameters that AAO surface areas are $1{,}225{,}220cm^2$, $320{,}442cm^2$, $54{,}997cm^2$, respectively. That means if an 1 cm^3 (surface area is $6cm^2$) sample has AAO structure the surface areas can increase to 204,203, 53,407, and 9,166 times. The large surface area of nanoporous AAO film enhances the adsorption of bromophenol blue indicator. The color of AAO film with bromophenol blue adsorption is sensitive to the pH. The indicator adsorbed AAO film can further be a precise measurement tip in the bio-technology, physical, or chemical applications.

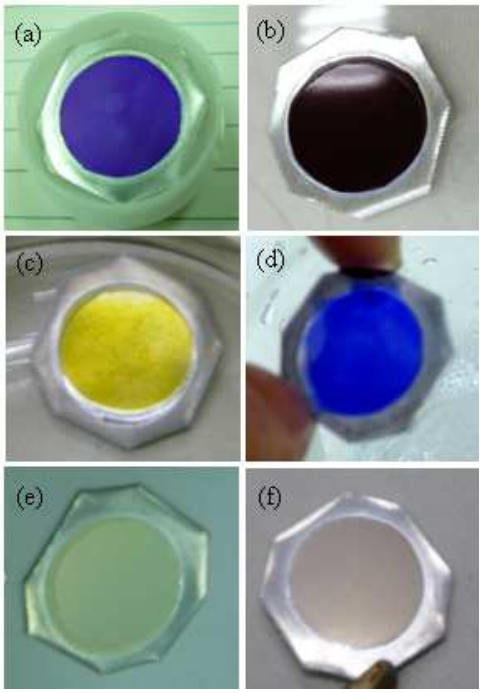

Fig. 4 Optical images of AAO surface colors. (a) blue color with AAO adsorbs bromophenol blue solution for a short time, (b) dark blue color with AAO absorbs bromophenol blue solution for a long time, (c) yellow color with AAO/ bromophenol blue tested in the acid solution, (d) light blue color with AAO/ bromophenol blue tested in the basic solution, (e) light yellow color with bromophenol blue removed by acetone dissolution, (f) gray color with bromophenol blue removed by heating.

Acknowledgment

This study was partially supported by a grant from the National Science Council, Ta05iwan (100-2918-I-239-001-).

References

[1] M.C. Roco,.,Journal of Nanoparticle Research 7, 707 (2005).
[2] C.C. Chen, W.D. Jehng, L.L. Li, W.G. Diau, J. Electrochemical Soci., 156, C304 (2009)
[3] C.C. Chen, H.W. Chung, C.H. Chen, H.P. Lu, C.M. Lan, S.F. Chen, L. Luo, C.S. Hung, E.W.G. Diau, J. Phys. Chem. C 112, 19151 (2008).
[4] Pribat, Didier; Cojocaru, Costel Sorin; Xavier, Stephane; Lim, Sung Hoon; Guilley, Arnaud Jullien; Legagneux, Pierre; Minoux, Eric, Digest of Technical Papers – SID International Symposium 38, 1409 (2007).
[5] Novak, J.F. (Applied Nanotech, Inc.); Fink, R.L.; Yaniv, Z., Proceedings of the 12th International Display Workshops in Conjunction with Asia Display 2005, 257 (2005).
[6] G. Jeon, S.Y. Yang, J. Byun, J.K. Kim, Nano Letters, 11, 1284 (2011).
[7] R. Keller and F. hunter: J. Electrochem. Soc. 100, (1953) 411.
[8] H. Lewis and L. Plumb: J. Electrochem., Soc. 105, 496 (1958).
[9] T. Edwards and R. Keller: Metals Technol., 11 Techn. Publ. 1, 710 (1944).
[10] K. T. Sunil and C. C.Hsueh: Chaos 12, 240 (2002).
[11] H. Masuda and F. Hasegwa: J. Electrochem. Soc. 144, 127 (1997).
[12] H. Masuda and K. Fukuda: Science 268, 1466 (1995).
[13] H. Masuda and M. Yotsuya: Appl. Phys. Lett. 78, 826 (2001).
[14] R. J. Tonucci and B, L. Justus: Science, 258, 783 (1992).
[15] R. Charles and H. Martin: Chem. Mater., 8, 1739 (1996).
[16] F. Burmeister and C. Schafle: Adv., Mater., 10, 495 (1998).
[17] H. Akahori: J. Electron Microscopy Japan 11, 217 (1962).
[18] R. Charles and S. Spooner: J. Electrochem. Soc. 102, 156 (1955).
[19] Setoh, S. Miyata, A., Sci. Pap. Inst. Phys. Chem. Res., Tokyo, 189(1932).
[20] Akahori, J. Electron microscopy, Japan, (1962).